

## MILLIMETER MULTIPLICITY IN NGC 6334 I AND I(N)

T.R. HUNTER<sup>1</sup>, C.L. BROGAN<sup>2</sup>, S.T. MEGEATH<sup>1,3</sup>, K.M. MENTEN<sup>4</sup>, H. BEUTHER<sup>5</sup>, S. THORWIRTH<sup>4</sup>

(Received 02 March 2006; Revised 14 May 2006; Accepted 17 May 2006)

## ABSTRACT

Using the Submillimeter Array (SMA), we have imaged the 1.3 millimeter continuum emission at the center of the massive star-forming regions NGC 6334 I and I(N). In both regions, the SMA observations resolve the emission into multiple millimeter sources, with most of the sources clustered into areas only 10,000 AU in diameter. Toward NGC 6334 I, we find four compact sources: the two brightest (I-SMA1 and I-SMA2) are associated with previously-known ammonia cores; I-SMA3 is coincident with the peak of the compact H II region (NGC 6334 F); and I-SMA4 is a newly-discovered object. While I-SMA3 exhibits a mixture of free-free and dust emission, the rest of the objects are dust cores. Toward NGC 6334 I(N), seven compact dust cores are found, one of which is associated with a faint centimeter source. With the exception of I-SMA3, none of the millimeter sources have infrared counterparts in *Spitzer* Space Telescope 3-8  $\mu\text{m}$  images. Using a simple physical model for the dust continuum emission, the estimated mass of interstellar material toward each of these compact objects is in the range of 3 to 66  $M_{\odot}$ . The total mass in the compact objects appears to be similar in I and I(N). The small size of these groups of sources suggest that these objects are proto-Trapezia forming in the centers of clusters of low to intermediate-mass stars.

*Subject headings:* stars: formation — infrared: stars — ISM: individual (NGC 6334 I) — ISM: individual (NGC 6334 I(N)) — techniques: interferometric — submillimeter

## 1. INTRODUCTION

The formation process of massive stars continues to be a poorly-understood phenomenon in astrophysics. The most fundamental clues to the origin of OB stars are their multiplicity and their common association with high column densities of molecular gas and dust. A unique feature of OB stars is that they are often found in non-hierarchical (and consequently) non-stable systems in the center of clusters (Sharpless 1954). A nearby example of this phenomenon is the Orion Trapezium with projected stellar separations of 4000 to 10000 AU, which in turn is found in the center of a rich cluster of low mass stars. A long-standing question is whether these multiple systems are the direct result of the formation process, thus providing a clue to the process of high mass star formation, or the result of dynamical evolution in the centers of young clusters where the most massive stars move toward the center by ejecting lower mass stars outward (Bonnell & Davies 1998). While recent (sub)millimeter studies have identified good candidates for massive protoclusters on scales of several parsecs, the identification of proto-Trapezia is a more difficult prospect. Due to the complex nature of high mass star-forming regions, the high extinction typically observed toward massive protostars, and their typically large distance ( $> 1$  kpc), high-resolution imaging at (sub)millimeter wavelengths is required to resolve one protostar from another. Recent space-based near-infrared (NIR) imaging has succeeded in identifying a

5600 AU diameter cluster of five proto-OB stars comprising W3 IRS 5 (Megeath et al. 2005). However, because massive protostars form in the deeply-embedded cores of molecular clouds, dust extinction may obscure a significant fraction of them in the infrared. In these cases, millimeter continuum emission from dust provides one of the few alternative tracers of protostars because it remains optically thin at high column densities ( $N_{\text{H}} \lesssim 10^{25} \text{cm}^{-2}$ ).

The recent commissioning of the Submillimeter Array (SMA) on Mauna Kea, Hawaii has expanded the range of millimeter interferometry to higher frequencies and lower declinations. Now within reach is NGC 6334 ( $\delta = -35^{\circ}$ ), a luminous and relatively nearby (1.7 kpc; Neckel 1978) molecular cloud/H II region complex containing several concentrations of massive star formation at various stages of evolution (Straw & Hyland 1989). The north-eastern end appears to be the youngest and contains the radio source “F” (G351.42+0.64; Rodríguez et al. (1982)) which is associated with IRAS 17175-3544. The earliest far-infrared images of this region (Emerson et al. 1973; McBreen et al. 1979) identified the emission as source “I”. An additional component “I(N)” was first detected at 1mm (Cheung et al. 1978) and later at 400 $\mu\text{m}$  (Gezari 1982). Further observations have demonstrated that although these two cores have comparable mass, NGC 6334 I dominates the combined bolometric luminosity of  $2.6 \times 10^5 L_{\odot}$  (Sandell 2000). In the NIR, an embedded cluster of stars has been detected in the central 2' of NGC 6334 I (Tapia et al. 1996). In contrast, the only NIR emission detected toward I(N) are H<sub>2</sub> knots that are most likely associated with outflow activity (see Figure 3 of Megeath & Tieftrunk (1999)). In this paper, we present the first 1.3 millimeter interferometry of NGC 6334 I and I(N). Despite their strikingly different appearance in the NIR, we find that both regions contain a similar cluster of compact dust continuum cores. A de-

Electronic address: thunter@cfa.harvard.edu

<sup>1</sup> Harvard-Smithsonian Center for Astrophysics, Cambridge, MA 02138<sup>2</sup> NRAO, 520 Edgemont Rd, Charlottesville, VA 22903<sup>3</sup> Ritter Observatory, MS 113, University of Toledo, Toledo, OH 43606-3390<sup>4</sup> MPIfR Bonn, Germany<sup>5</sup> MPIA Heidelberg, Germany

tailed treatment of the millimeter line emission accompanying these objects will be the subject of a forthcoming paper (Hunter et al., in preparation).

## 2. OBSERVATIONS

### 2.1. Submillimeter Array (SMA)

The SMA<sup>6</sup> observations were made with six antennas in both the compact configuration (2004 May), and extended configuration (2005 May). Two pointings were observed: NGC 6334 I at  $17^{\text{h}}20^{\text{m}}53^{\text{s}}.44$ ,  $-35^{\circ}47'02''.2$  and NGC 6334 I(N) at  $17^{\text{h}}20^{\text{m}}54^{\text{s}}.63$ ,  $-35^{\circ}45'08''.5$  (J2000). Unprojected baseline lengths ranged from 22m to 226m. The SMA receivers are double sideband mixers with 2 GHz bandwidth (Blundell 2004). The center frequencies were 217.6 in LSB and 227.6 GHz in USB. The correlator was configured for uniform resolution (0.81 MHz per channel). Typical system temperatures were 200K. The gain calibrators were NRAO 530 (23° distant) and J1924–292 (27° distant) and the band-pass calibrators were Uranus and 3C279. The data were calibrated in Miriad, then exported to AIPS where the line and continuum emission were separated with the task UVLSF. Self-calibration was performed on the continuum data, and solutions were transferred to the line data. Flux calibration is based on SMA flux monitoring of the observed quasar and is estimated to be accurate to within 20%. The estimated accuracy of the absolute coordinates is  $0.4''$ . After combining the calibrated LSB and USB continuum uv-data, the  $1\sigma$  rms noise level achieved in the continuum images is  $7 \text{ mJy beam}^{-1}$ . The resulting synthesized beam is  $2''.1 \times 1''.2$  and the primary beam is  $\sim 56''$ .

### 2.2. Very Large Array (VLA)

Archival 3.6 cm data from the NRAO<sup>7</sup> Very Large Array (VLA) were calibrated and imaged in AIPS. The observation date was May 7, 1990 (A-configuration). The flux calibrator was 3C286, and the gain calibrator was NRAO530. The synthesized beam of the 3.6 cm continuum image is  $0.90'' \times 0.43''$  at (P.A. =  $-18^{\circ}$ ) and the rms sensitivity is  $1 \text{ mJy beam}^{-1}$ .

### 2.3. Spitzer Space Telescope

Both SMA fields were observed with the IRAC camera (Fazio et al. 2004) onboard the *Spitzer* Space Telescope. The total integration time was 666 seconds. The high dynamic range mode was used to obtain 0.4 and 10.4 second integrations. The data were reduced using the BCD data from the Spitzer Science Center version 11.4 pipeline. When constructing images, the 0.4 second data were used toward pixels where the 10.4 second data were saturated, which is only the case for some of the sources in NGC 6334 I. The pixel size for the images is  $1''.2$ . Upper limits were derived from mosaics produced with the MOPEX program. To calculate the upper limits, the rms signal was found for a  $5 \times 5$  pixel box centered on

the SMA sources. These values were converted to units of mJy per pixel, then multiplied by a factor of 5/2 to calculate  $5\sigma$  limits for detections in a  $2 \times 2$  pixel aperture.

## 3. RESULTS

### 3.1. NGC 6334 I

The 1.3 mm continuum emission in NGC 6334 I is shown in Figure 1. We have resolved four major continuum sources which we denote as I-SMA1..4, in descending order of peak intensity (see Table 1). The continuum sources are all fairly compact. Gaussian fitting yields formal size estimates between 1.6 and 2.7 arcsec (2800 and 4600 AU). Including compact and extended emission, the total flux density within Figure 1 is  $10.7 \pm 0.1 \text{ Jy}$ , equivalent to  $43 \pm 5\%$  of the single dish continuum flux density (Sandell 2000). The overall extent of the emission ( $\approx 10''$ ) agrees well with the size estimate from single-dish maps (Sandell 2000). No other sources are found beyond this central concentration of objects. The two brightest millimeter sources (I-SMA1 and I-SMA2) correspond within  $0.5''$  to the two primary  $\text{NH}_3$  peaks observed in the (1,1), (2,2), and (3,3) transitions (Beuther et al. 2005; Kraemer & Jackson 1995). The  $\text{H}_2\text{O}$  masers form a linear structure (Forster 1992) that appears to be associated with I-SMA1. In contrast, the 6.7 GHz  $\text{CH}_3\text{OH}$  masers are associated with I-SMA2 and I-SMA3. I-SMA3 coincides to within  $0.3''$  of the peak of the 3.6 cm emission which traces a cometary compact H II region (Carral et al. 1997). Based on the 3.6 cm flux density, we estimate that the free-free contribution to the 1.3 mm flux density of I-SMA3 is  $\sim 1.25 \text{ Jy}$  (62%). The rest of the 1.3 mm continuum emission from this source (and all of the other sources) originates from dust. I-SMA3 lies  $1.0''$  south of the NIR star IRS1E which has been proposed as the exciting source of the compact H II region (Persi et al. 1996). Since free-free emission dominates I-SMA3, it is perhaps not surprising that its position lies closer to the mid-IR/cm peak than to IRS1E. The known mid-IR sources IRS-I 2 (Persi et al. 1998) and DPT00 2 (De Buizer et al. 2002) reside within the extended millimeter contours, but the lack of a compact millimeter source at these positions supports the hypothesis of De Buizer et al. (2002) that they are not internally heated. With the exception of the H II region nebula (I-SMA3), none of the millimeter sources are detected in the IRAC images. Indeed, no compact counterpart at any other wavelength has been observed toward I-SMA4.

### 3.2. NGC 6334 I(N)

We have resolved the millimeter continuum of NGC 6334 I(N) into seven sources, which we denote as I(N)-SMA1..7 (Figure 2). Including the extended emission, the fraction of single-dish flux recovered in our image is  $32 \pm 8\%$ . Nearly half of the total emission originates from I(N)-SMA1. Although this field lacks any strong centimeter continuum emission, two faint 3.6 cm (0.3 mJy) sources have been reported (Carral et al. 2002). One of these sources lies within  $0.6''$  of I(N)-SMA4, which is also the source closest to a Class II  $\text{CH}_3\text{OH}$  maser (Walsh et al. 1998; Norris et al. 1993). The faint continuum source with its (probable) associated class II  $\text{CH}_3\text{OH}$  maser may represent a hypercompact H III region, similar to the sources found by

<sup>6</sup> The Submillimeter Array (SMA) is a collaborative project between the Smithsonian Astrophysical Observatory and the Academia Sinica Institute of Astronomy & Astrophysics of Taiwan.

<sup>7</sup> The National Radio Astronomy Observatory is a facility of the National Science Foundation operated under agreement by the Associated Universities, Inc.

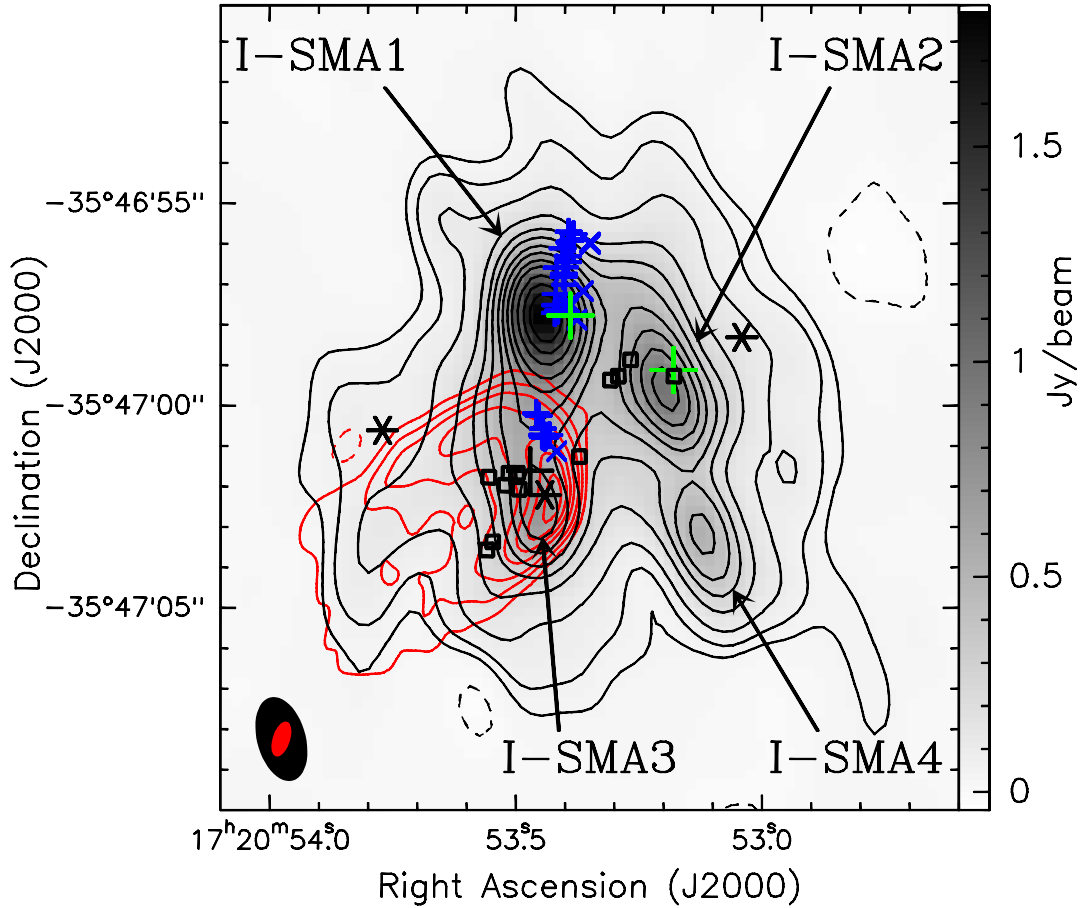


FIG. 1.— *Grayscale and black contours*: 1.3mm continuum image of NGC 6334 I taken from the combined LSB plus USB data. Contour levels are  $(-3, 3, 6, 12, 18, 24, 36, 48, 64, 80, 100, 120, 150, 180) \times 7.5$  mJy/beam. Water masers are marked by the blue symbols: 'x' (Migenes et al. 1999) and '+' (Forster 1992) (shifted by the amount suggested in a private communication from J. Forster in Carral et al. (1997)). Open squares mark Class II CH<sub>3</sub>OH masers (Walsh et al. 1998). The black cross marks IRS 1E and the six-pointed stars mark the three mid-infrared sources from east to west: DPT00 2 (De Buizer et al. 2000), IRS-I 1 and IRS-I 2 (De Buizer et al. 2002). The green crosses mark NH<sub>3</sub> peaks (derived from images of the hyperfine lines of Beuther et al. (2005)). *Red contours*: VLA 3.6 cm emission ( $-5, 5, 15, 30, 60, 90, 120, 150$  mJy beam<sup>-1</sup>).

TABLE 1  
PROPERTIES OF MILLIMETER CONTINUUM SOURCES IN NGC 6334 I AND I(N)

Source	J2000 coordinates		$I_{1.3\text{mm}}$ (Jy/b)	$F_{1.3\text{mm}}$ (Jy)	$F_{4.5\mu\text{m}}$ (mJy)	$F_{8.0\mu\text{m}}$ (mJy)
	$\alpha$ (h m s)	$\delta$ (° ' ")				
I-SMA1	17 20 53.44	-35 46 57.9	1.77	$3.49 \pm 0.70$	$< 320$	.. <sup>a</sup>
I-SMA2	17 20 53.20	-35 46 59.6	0.96	$2.28 \pm 0.46$	$< 240$	$< 1490$
I-SMA3	17 20 53.45	-35 47 02.6	0.71	$2.01 \pm 0.40$	.. <sup>a</sup>	.. <sup>a</sup>
I-SMA4	17 20 53.12	-35 47 03.2	0.52	$1.10 \pm 0.22$	$< 260$	$< 1490$
Total				$10.7 \pm 2.1^b$		
I(N)-SMA1	17 20 55.21	-35 45 04.1	0.82	$2.04 \pm 0.41$	$< 0.11$	$< 0.71$
I(N)-SMA2	17 20 54.90	-35 45 06.8	0.35	$0.50 \pm 0.10$	$< 0.35$	$< 0.53$
I(N)-SMA3	17 20 55.00	-35 45 07.5	0.27	$0.39 \pm 0.09$	$< 0.21$	$< 0.53$
I(N)-SMA4	17 20 54.69	-35 45 08.5	0.17	$0.33 \pm 0.07$	$< 0.70$	$< 0.77$
I(N)-SMA5	17 20 55.08	-35 45 02.0	0.27	$0.28 \pm 0.07$	$< 0.12$	$< 0.63$
I(N)-SMA6	17 20 54.59	-35 45 17.9	0.27	$0.47 \pm 0.10$	$< 0.29$	$< 0.69$
I(N)-SMA7	17 20 54.96	-35 44 57.3	0.07	$0.20 \pm 0.05$	$< 0.51$	$< 0.68$
I(N) Total				$4.6 \pm 0.9^b$		

<sup>a</sup> The extended nebula of the compact HII region precludes a meaningful infrared point source upper limit

<sup>b</sup> The total 1.3mm flux density includes the extended emission; the listed uncertainties include 20% calibration uncertainty

van der Tak & Menten (2005) in other massive star formation regions. If this interpretation is true, then this object is an important power source in the I(N) region. Class I CH<sub>3</sub>OH masers have also been identified in this

region at 25 GHz (Beuther et al. 2005) and at 44 GHz but with uncertain astrometry (Kogan & Slysh 1998). None of the millimeter sources have counterparts in our IRAC data ( $5\sigma$  upper limits at  $4.5\mu\text{m}$  and  $8\mu\text{m}$  are given

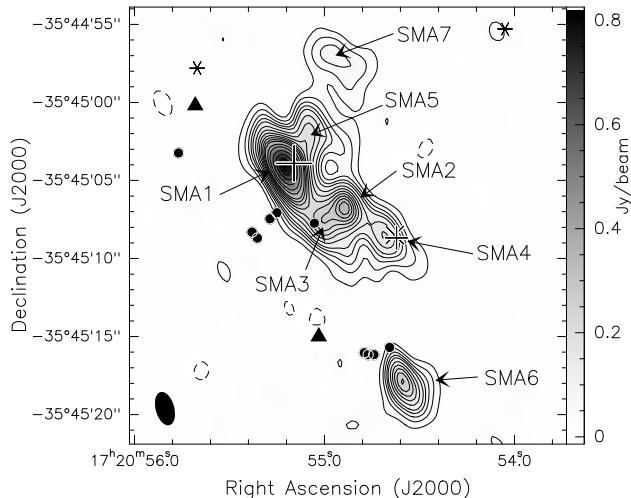


FIG. 2.— 1.3 mm continuum image of NGC 6334 I(N). Contour levels are (-3, 3, 6, 9, 12, 15, 20, 25, 30, 35, 40, 45, 50, 60, 70, 85, 100, 115)  $\times$  6.5 mJy/beam. Filled circles mark 44 GHz Class I  $\text{CH}_3\text{OH}$  masers (Kogan & Slysh 1998), the small cross marks a 6.7 GHz Class II  $\text{CH}_3\text{OH}$  maser (Norris et al. 1993; Walsh et al. 1998), the X marks the faint 3.6 cm source (Carral et al. 2002), and the 6-pointed stars mark infrared  $\text{H}_2$  knots (Megeath & Tieftrunk 1999). The filled triangles mark 25 GHz Class I  $\text{CH}_3\text{OH}$  masers and the large cross indicates the  $\text{NH}_3$  peak (Beuther et al. 2005).

in Table 1). However, directly west of I(N)-SMA4 is an extended infrared source detected at 4.5 and 5.8  $\mu\text{m}$  (Figure 3). The elongated morphology suggests a jet or a reddened reflection nebulosity from an outflow cavity. In either scenario, the extended mid-IR emission would be the result of outflow activity from the embedded source in I(N)-SMA4. The unipolarity could be explained if the other lobe of the putative outflow was obscured by stronger extinction in its direction. This possible association is the only evidence, albeit indirect, for the I(N)-SMA sources at wavelengths  $\leq 8 \mu\text{m}$ .

### 3.3. Mass estimates from the dust emission

We can estimate the mass of the individual dust sources by placing our millimeter continuum measurements in the context of a simple isothermal model of optically-thin dust emission (Beltrán et al. 2006). The assumption of low optical depth is justified because the peak continuum brightness temperature of the strongest dust source (I-SMA1) is only 6.3 K. The input parameters to the model include the dust temperature, the dust mass opacity coefficient at the observed wavelength ( $\kappa_{1.3\text{mm}}$ ), and the gas-to-dust mass ratio. Based on our SMA spectra (Hunter et al., in preparation), we can categorize the sources into three groups: A) strong hot-core line emission: I-SMA1, I-SMA2 and I(N)-SMA1, B) weak line emission: I-SMA3 and I(N)-SMA2, and C) nearly line-free emission. Thus, from a qualitative viewpoint, the gas and dust is likely to be warmest in the group A sources, and coolest in the group C sources. By combining this information with the various gas temperature measurements from the literature, we have assigned a probable value for the dust temperature of each source including upper and lower limits (see Table 2).

For the sources in group A, the brightness temperature of the arcsecond scale  $\text{NH}_3$  (2,2) emission provides the lower-limit temperature (Beuther et al. 2005). For

TABLE 2  
RANGE OF ESTIMATED TEMPERATURES AND MASSES OF DUST CORES IN NGC 6334 I AND I(N)

Source	$\kappa$ ( $\text{cm}^2 \text{g}^{-1}$ )	cold limit		nominal		warm limit	
		$T$ (K)	$M$ ( $M_\odot$ )	$T$ (K)	$M$ ( $M_\odot$ )	$T$ (K)	$M$ ( $M_\odot$ )
I-SMA1	2	75	23	100	17	300	5.4
I-SMA2	2	75	15	100	11	300	3.5
I-SMA3	1	40	52	60	33	100	19
I-SMA4	1	20	66	33	36	50	22
Total			156		97		50
I(N)-SMA1	2	65	15	100	10	300	3.1
I(N)-SMA2	1	20	30	40	13	100	4.8
I(N)-SMA3	1	20	23	33	13	50	7.8
I(N)-SMA4	1	20	20	33	11	50	6.1
I(N)-SMA5	1	20	17	33	9	50	5.2
I(N)-SMA6	1	20	28	33	15	50	8.7
I(N)-SMA7	1	20	12	33	6	50	3.7
I(N) Total			145		77		39

I-SMA1 and I-SMA2, we set the “nominal” temperature equal to the dust temperature (100 K) obtained from fits to the single-dish spectral energy distribution (SED) for source I (Sandell 2000). We also use 100 K for I(N)-SMA1, because the single-dish intensity ratio of  $\text{NH}_3$  (6,6) to (3,3) indicates the presence of gas with  $T > 95$  K (Kuiper et al. 1995); furthermore, recent interferometric measurements have localized the bulk of the  $\text{NH}_3$  (6,6) emission to the position of I(N)-SMA1 (Beuther et al., in preparation). For an upper limit temperature for group A, we adopt 300 K because an excitation temperature of 295 K was measured for  $\text{H}_2\text{CO}$  in NGC 6334 I by Mangum & Wootten (1993) and 213 K for  $\text{CH}_3\text{OH}$  by van der Tak et al. (2003). For the sources in group B, we set the nominal temperature equal to the CO excitation temperature derived by Kraemer et al. (1999) which is 60 K for NGC 6334 I and 40 K for I(N). For the sources in group C, we set the nominal temperature equal to the value (33 K) derived from a Large Velocity Gradient analysis of a single-dish submillimeter line survey (McCutcheon et al. 2000). In both I and I(N), the lower limit temperature of the group B and C sources is taken to be the temperature of the coolest dust core (20 K) in the surrounding region as measured by Sandell (2000), while the upper limit is taken to be 50 K due to the lack of direct evidence of any warmer gas at these positions. Measurements of  $\kappa_{1.3\text{mm}}$  in NGC 6334 I and I(N) with a 30'' beam yield values from 1.0 to  $1.2 \pm 0.6 \text{ cm}^2 \text{g}^{-1}$  (Schwartz et al. 1989). However, due to the large range of temperature in the compact millimeter sources, we have chosen to use tabulated values of  $\kappa_{1.3\text{mm}}$  from Ossenkopf & Henning (1994) for a density of  $10^6 \text{ cm}^{-3}$ . For sources in group A, we use a  $\kappa_{1.3\text{mm}} = 2 \text{ cm}^2 \text{g}^{-1}$  for dust grains without mantles, which is appropriate for regions where protostellar heating has destroyed the solid ice but has not yet dispersed the dust aggregates. In the other millimeter sources which show no hot core emission and are opaque at infrared wavelengths, the grains are likely to have thick ice mantles; thus we use  $\kappa_{1.3\text{mm}} = 1 \text{ cm}^2 \text{g}^{-1}$ . Applying a gas-to-dust mass ratio ( $g$ ) of 100 (Sodroski et al. 1997), these assumptions yield the masses listed in Table 2. Due to uncertainties in  $\kappa_{1.3\text{mm}}$  and  $g$ , the uncertainties in all

of the masses in Table 2 are likely to be at least a factor of two. Subject to these uncertainties, the total mass estimates of the compact objects (in both the warm and cold temperature limits) are of similar magnitude in I and I(N), ranging from  $\sim 50 M_{\odot}$  to  $\sim 150 M_{\odot}$ . In I(N), this mass is divided among a larger number sources which are, in turn, spread over a larger angular extent.

#### 4. DISCUSSION

The observed multiplicity and strength of the millimeter continuum emission is quite similar between NGC 6334 I and I(N), in contrast to their strikingly different appearance in the NIR (Megeath & Tieftrunk 1999) and in thermal lines of  $\text{NH}_3$  and  $\text{CH}_3\text{OH}$  (Beuther et al. 2005). Although previous maser and  $\text{NH}_3$  observations of NGC 6334 I had suggested the presence of multiple sources, our millimeter image provides a direct and unambiguous picture of a massive protocluster. The estimated mass of interstellar material toward each source is sufficient to form a massive star and is significantly greater than typical objects detected in the single-dish surveys of low-mass star-forming regions such as Perseus, where an average core mass of  $2.3 M_{\odot}$  has been found with a beamsize of  $\sim 8000$  AU (Enoch et al. 2006). In addition, it is likely that a compact protostellar object may already be present at the center of each source, heating the surrounding gas and dust and leading to our strong millimeter detections. This scenario is particularly likely for the strong hot-core sources I-SMA1 and I-SMA2. It is important to note that the masses in Table 2 do not include the total stellar mass that may be present in addition to the interstellar material.

In the case of NGC 6334 I(N), the presence of outflows, masers, warm gas emission, and a faint centimeter continuum source also indicates the presence of embedded sources. In comparison to source I, this cluster of sources may be in an earlier evolutionary phase, as suggested by the lack of a NIR cluster, HII region, or bright mid-IR source, and the significantly higher gas column density inferred from  $\text{N}_2\text{H}^+$  observations (Pirogov et al. 2003). However, if the millimeter sources contain central protostars, then the lack of mid-IR detections toward all seven sources is especially curious, because, in contrast to source I, there is no confusion from bright, extended nebulosity in this region. If we consider the I(N) bolometric luminosity of  $1.9 \times 10^3 L_{\odot}$  (Sandell 2000), the earliest ZAMS star that could be present is type B2V (Hanson et al. 1997). Our lowest  $4.5\mu\text{m}$  upper limit of 0.11 mJy (from Table 1) corresponds to an apparent magnitude  $m_{4.5\mu\text{m}} > 15.5$ . This limit is consistent with the non-detection of an embedded B2V ZAMS star as long as the extinction at  $4.5\mu\text{m}$  is  $\geq 4.9$  mag, assuming an absolute stellar magnitude of  $M_K = -0.68$  (Hanson et al. 1997) and an intrinsic color  $(M_K - M_{4.5\mu\text{m}}) = -0.08$  mag (Koornneef 1983). This level of extinction at  $4.5\mu\text{m}$  corresponds to 9.3 mag of  $K$  band extinction (Indebetouw et al. 2005), 83 mag of  $V$  band extinction (Rieke & Lebofsky 1985), and a total hydrogen column density of  $1.8 \times 10^{23} \text{ cm}^{-2}$  (Ryter 1996). Even using the smallest mass estimates from Table 2, the gas column density implied by the dust emission is several times larger than this value and can easily explain the non-detections. As a result, it is unclear whether these millimeter sources contain young protostars (B2 or

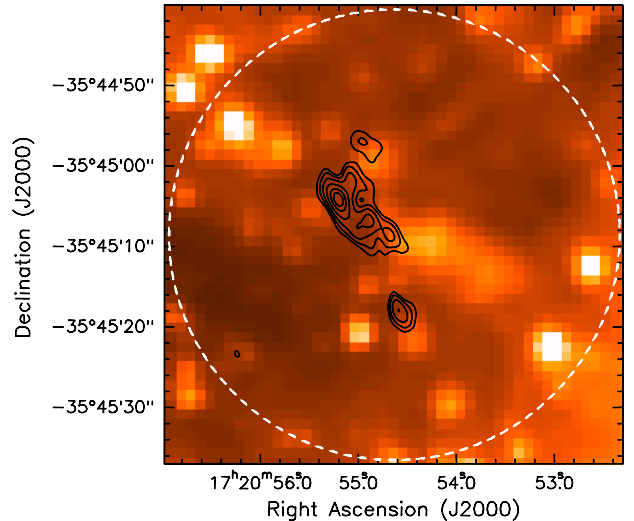


FIG. 3.—  $4.5\mu\text{m}$  IRAC image of NGC 6334 I(N). Contours indicate the 1.3mm continuum emission (5, 10, 20, 40, 70, 100  $\times$  6.5 mJy/beam) and the dashed circle shows the primary beam of the 1.3mm SMA observations. The newly-detected infrared nebula happens to lie near the center of this circle, just west of I(N)-SMA4.

later) that are simply heavily obscured, or whether they are intrinsically faint in the mid-IR due to their youth, and may eventually evolve into higher luminosity O stars. In either case, the high angular resolution and sensitivity of our observations have revealed the presence of compact systems where intermediate to high mass stars are being formed.

In NGC 6334 I, all four of the compact millimeter continuum sources are concentrated within a region of projected radius  $\leq 0.05$  pc which is significantly smaller than the 0.33 pc radius of the NIR cluster (Tapia et al. 1996) and the 0.23 pc radius of the search region (i.e. the SMA primary beam). Furthermore, the millimeter sources in NGC 6334 I reside close to the geometric center of the NIR cluster where the number density of millimeter sources ( $8000 \text{ pc}^{-3}$ ) exceeds the stellar density of the NIR cluster ( $1200 \text{ pc}^{-3}$ ). These findings suggest that massive star formation is biased toward the center of the parent cluster. The projected separation of the four components of NGC 6334 I range from 5800 to 11200 AU. Because the ratio of distances between all components is less than three, it satisfies the criterion for identifying Trapezia as described by Abt & Corbally (2000) and originated by Ambartsumian (1954). If the total luminosity of NGC 6334 I ( $2.6 \times 10^5 L_{\odot}$ ) was apportioned equally to four sources, their individual luminosities would correspond to that of an O8.5 ZAMS star (Hanson et al. 1997). These findings argue that the NGC 6334 I SMA sources may constitute a proto-Trapezium system, similar to the more evolved Orion Nebula Trapezium (10,000 AU in diameter) and many other optically visible nebulae and clusters. Although the I(N) SMA sources are more spread out, five of the sources of I(N) reside inside a region of 10,000 AU, suggesting that a similar system is forming in I(N). These observations suggest that the presence of Trapezia in clusters and nebulae may result from the massive stars forming preferentially in the centers of clusters in the deepest part

of the gravitational well.

Are these new observations consistent with previous claims (Megeath & Tieftrunk 1999; Sollins & Megeath 2004) that NGC 6334 I(N) is in an earlier stage of star formation? In source I, we have identified examples of young massive protostars in the center of an established infrared cluster containing low to intermediate mass stars. In source I(N), we see evidence of massive protostars without a surrounding NIR cluster, which challenges the common picture of high mass stars forming after the first generation of low mass stars (e.g. Herbig (1962); Kumar et al. (2006)). More sensitive infrared imaging is needed to probe deeper through the extinction for signs of lower mass protostars in this field. However, until such evidence is found, the question of the relative age of I and I(N) hinges on three main facts: 1) the ratio of bolometric luminosity between I and I(N) is large ( $\approx 140$ ) (Sandell 2000); 2) the I(N) region exhibits significantly less hot-core line emission than NGC 6334 I (Thorwirth et al. (2003); Hunter et al., in preparation); 3) a cluster of compact dust continuum sources exists in I and I(N) with a comparable amount of mass (this paper). These observations suggest that NGC 6334 I is a more evolved cluster than I(N), or that I(N) is forming a cluster with a larger number of stars but of lower mass. In either case, our millimeter data provide strong evidence that NGC 6334 I(N) is forming a cluster of stars, even though an associated NIR cluster has not been identified, and may be still in the process of forming. Finally,

we note that the virial masses derived from single-dish molecular line spectra (including  $N_2H^+$  by Pirogov et al. (2003) and  $HC_3N$  by Sollins & Megeath (2004)) for both NGC 6334 I and I(N) are several times higher than the total estimated mass contained in the compact millimeter sources. This fact illustrates the wealth of star-forming material in both regions that has either not assembled into compact protostars or exists in a wider distribution of smaller cores below our sensitivity limit. It is this gas which may be forming the cluster surrounding the SMA sources in NGC 6334 I(N) and which may further increase the population of the cluster in NGC 6334 I.

The authors wish to thank the anonymous referee for a diligent report which improved this manuscript. This work is based in part on observations made with the *Spitzer* Space Telescope, which is operated by the Jet Propulsion Laboratory, California Institute of Technology under a contract with NASA. This research has made use of NASA's Astrophysics Data System Bibliographic Services and the SIMBAD database operated at CDS, Strasbourg, France. Support for STM was provided by NASA through contract 1256790 issued by JPL/Caltech. HB acknowledges financial support by the Emmy-Noether-Program of the Deutsche Forschungsgemeinschaft (DFG, grant BE2578).

#### REFERENCES

- Abt, H. A. & Corbally, C. J. 2000, *ApJ*, 541, 841  
 Ambartsumian, V. A. 1954, *Les Processus Nucléaires dans les Astres*, 293  
 Beltrán, M. T., Brand, J., Cesaroni, R., Fontani, F., Pezzuto, S., Testi, L., & Molinari, S. 2006, *A&A*, 447, 221  
 Beuther, H., Thorwirth, S., Zhang, Q., Hunter, T. R., Megeath, S. T., Walsh, A. J., & Menten, K. M. 2005, *ApJ*, 627, 834  
 Blundell, R. 2004, in *Proceedings of the 15th International Symposium on Space Terahertz Technology*, 3  
 Bonnell, I. A., & Davies, M. B. 1998, *MNRAS*, 295, 691  
 Carral, P., Kurtz, S. E., Rodríguez, L. F., de Pree, C., & Hofner, P. 1997, *ApJ*, 486, L103+  
 Carral, P., Kurtz, S. E., Rodríguez, L. F., Menten, K., Cantó, J., & Arceo, R. 2002, *AJ*, 123, 2574  
 Cheung, L., Frogel, J. A., Hauser, M. G., & Gezari, D. Y., *ApJ*, 226, L149  
 De Buizer, J. M., Piña, R. K., & Telesco, C. M. 2000, *ApJS*, 130, 437  
 De Buizer, J. M., Radomski, J. T., Piña, R. K., & Telesco, C. M. 2002, *ApJ*, 580, 305  
 Emerson, J. P., Jennings, R. E., & Moorwood, A. F. M. 1973, *ApJ*, 184, 401  
 Enoch, M. L., et al. 2006, *ApJ*, 638, 293  
 Fazio, G. G. et al. 2004, *ApJS*, 154, 10  
 Forster, J. 1992, in *Astrophysical Masers*, ed. A. Clegg & G. Nedoluha (Springer-Verlag)  
 Gezari, D. Y. 1982, *ApJ*, 259, L29  
 Hanson, M. M., Howarth, I. D., & Conti, P. S. 1997, *ApJ*, 489, 698  
 Herbig, G. H. 1962, *Advances in Astronomy and Astrophysics*, 1, 47  
 Indebetouw, R., et al. 2005, *ApJ*, 619, 931  
 Kogan, L. & Slysh, V. 1998, *ApJ*, 497, 800  
 Koornneef, J. 1983, *A&A*, 128, 84  
 Kraemer, K. E. & Jackson, J. M. 1995, *ApJ*, 439, L9  
 Kraemer, K. E., Deutsch, L. K., Jackson, J. M., Hora, J. L., Fazio, G. G., Hoffmann, W. F., & Dayal, A. 1999, *ApJ*, 516, 817  
 Kuiper, T. B. H., Peters, W. L., Forster, J. R., Gardner, F. F., & Whiteoak, J. B. 1995, *ApJ*, 446, 692  
 Kumar, M. S. N., Keto, E., & Clerkin, E. 2006, *A&A*, 449, 1033  
 Mangum, J. G. & Wootten, A. 1993, *ApJS*, 89, 123  
 McBreen, B., Fazio, G. G., Stier, M., & Wright, E. L. 1979, *ApJ*, 232, L138  
 McCutcheon, W. H., Sandell, G., Matthews, H. E., Kuiper, T. B. H., Sutton, E. C., Danchi, W. C., & Sato, T. 2000, *MNRAS*, 316, 152  
 Megeath, S. T. & Tieftrunk, A. R. 1999, *ApJ*, 526, L113  
 Megeath, S. T., Wilson, T. L., & Corbin, M. R. 2005, *ApJ*, 622, L141  
 Migenes, V., Horiuchi, S., Slysh, V. I., Val'tts, I. E., Golubev, V. V., Edwards, P. G., Fomalont, E. B., Okayasu, R., Diamond, P. J., Umemoto, T., Shibata, K. M., & Inoue, M. 1999, *ApJS*, 123, 487  
 Neckel, T. 1978, *A&A*, 69, 51  
 Norris, R. P., Whiteoak, J. B., Caswell, J. L., Wieringa, M. H., & Gough, R. G. 1993, *ApJ*, 412, 222  
 Ossenkopf, V. & Henning, T. 1994, *A&A*, 291, 943  
 Persi, P., Roth, M., Tapia, M., Marenzi, A. R., Felli, M., Testi, L., & Ferrari-Toniolo, M. 1996, *A&A*, 307, 591  
 Persi, P., Tapia, M., Felli, M., Lagage, P. O., & Ferrari-Toniolo, M. 1998, *A&A*, 336, 1024  
 Pirogov, L., Zinchenko, I., Caselli, P., Johansson, L. E. B., & Myers, P. C. 2003, *A&A*, 405, 639  
 Rieke, G. H., & Lebofsky, M. J. 1985, *ApJ*, 288, 618  
 Rodríguez, L. F., Canto, J., & Moran, J. M. 1982, *ApJ*, 255, 103  
 Rytter, C. E. 1996, *Ap&SS*, 236, 285  
 Sandell, G. 2000, *A&A*, 358, 242  
 Schwartz, P. R., Snell, R. L., & Schloerb, F. P. 1989, *ApJ*, 336, 519  
 Sharpless, S. 1954, *ApJ*, 119, 334  
 Sodroski, T. J., Odegard, N., Arendt, R. G., Dwek, E., Weiland, J. L., Hauser, M. G., & Kelsall, T. 1997, *ApJ*, 480, 173  
 Sollins, P. K., & Megeath, S. T. 2004, *AJ*, 128, 2374  
 Straw, S. M. & Hyland, A. R. 1989, *ApJ*, 340, 318  
 Tapia, M., Persi, P., & Roth, M. 1996, *A&A*, 316, 102  
 Thorwirth, S., Winnemissner, G., Megeath, S. T., & Tieftrunk, A. R. 2003, in *ASP Conf. Ser. 287: Galactic Star Formation Across the Stellar Mass Spectrum*, 257–260  
 van der Tak, F. F. S., Boonman, A. M. S., Braakman, R., & van Dishoeck, E. F. 2003, *A&A*, 412, 133  
 van der Tak, F. F. S., & Menten, K. M. 2005, *A&A*, 437, 947  
 Walsh, A. J., Burton, M. G., Hyland, A. R., & Robinson, G. 1998, *MNRAS*, 301, 640